

SelT, SelW, SelH, and Rdx12: Genomics and Molecular Insights into the Functions of Selenoproteins of a Novel Thioredoxin-like Family[†]

Alexander Dikiy,^{‡,§} Sergey V. Novoselov,[‡] Dmitri E. Fomenko,[‡] Aniruddha Sengupta,^{||} Bradley A. Carlson,^{||} Ronald L. Cerny,[⊥] Krzysztof Ginalski,^{#,▽} Nick V. Grishin,[#] Dolph L. Hatfield,^{||} and Vadim N. Gladyshev^{*,‡}

Department of Biochemistry, University of Nebraska, Lincoln, Nebraska 68588, Molecular Biology of Selenium Section, Laboratory of Cancer Prevention, Center for Cancer Research, National Cancer Institute, National Institutes of Health, Bethesda, Maryland 20892, Department of Chemistry, University of Nebraska, Lincoln, Nebraska 68588, University of Texas Southwestern Medical Center, 5323 Harry Hines Boulevard, Dallas, Texas 75390, Interdisciplinary Centre for Mathematical and Computational Modelling, Warsaw University, Pawinskiego 5a, 02-106 Warsaw, Poland, and Department of Biotechnology, NTNU, 7491 Trondheim, Norway

Received November 30, 2006; Revised Manuscript Received March 30, 2007

ABSTRACT: Selenium is an essential trace element in many life forms due to its occurrence as a selenocysteine (Sec) residue in selenoproteins. The majority of mammalian selenoproteins, however, have no known function. Herein, we performed extensive sequence similarity searches to define and characterize a new protein family, designated Rdx, that includes mammalian selenoproteins SelW, SelV, SelT and SelH, bacterial SelW-like proteins and cysteine-containing proteins of unknown function in all three domains of life. An additional member of this family is a mammalian cysteine-containing protein, designated Rdx12, and its fish selenoprotein orthologue. Rdx proteins are proposed to possess a thioredoxin-like fold and a conserved CxxC or CxxU (U is Sec) motif, suggesting a redox function. We cloned and characterized three mammalian members of this family, which showed distinct expression patterns in mouse tissues and different localization patterns in cells transfected with the corresponding GFP fusion proteins. By analogy to thioredoxin, Rdx proteins can use catalytic cysteine (or Sec) to form transient mixed disulfides with substrate proteins. We employed this property to identify cellular targets of Rdx proteins using affinity columns containing mutant versions of these proteins. Rdx12 was found to interact with glutathione peroxidase 1, whereas 14-3-3 protein was identified as one of the targets of mammalian SelW, suggesting a mechanism for redox regulation of the 14-3-3 family of proteins.

Selenium is a trace element with significant biomedical potential (1). It has an essential role in mammals due to its occurrence in selenium-containing proteins, selenoproteins (2–5). Selenium is present in these proteins in the form of selenocysteine (Sec¹), which is the 21st amino acid in the genetic code. The overall composition of selenoproteomes (full set of selenoproteins in an organism) differs in major

domains of life, and the differences may even be seen between related species (6). Several animal selenoproteomes have previously been characterized. The human selenoproteome consists of 25 known selenoproteins, and mice and rats have 24 selenoproteins (7). About a third of these proteins participate in various redox reactions, whereas the functions of most other selenoproteins are not known. In order to explain the biomedical properties of dietary selenium, it is important to determine the functions of all selenoproteins.

Several mammalian selenoproteins have a conserved cysteine (Cys) in the vicinity of Sec, and these two residues are often organized in the form of a Cys-x-x-U (where U is Sec and x is any amino acid) motif. For example, this feature is present in mammalian SelT, SelW, SelV, SelH, and SelM, all of which are selenoproteins of unknown function. Of these, SelW was discovered first and is a better characterized protein (8). At 89 amino acids in length, it is the smallest mammalian selenoprotein expressed in various tissues and organs. SelW occurs in several protein forms due to posttranslational modifications, including glutathionylation and an unknown modification that adds 65 Da to its mass (8–11). SelW is particularly abundant in muscle, and its deficiency has been implicated in white muscle disease (12).

[†] This study was supported by NIH Grant GM061603 (to V.N.G.). It was completed in part utilizing the PrairieFire Beowulf cluster from Research Computing Facility at UNL, and the UNL mass spectrometry facility supported by NIH RR015468 and the Nebraska Research Initiative. This study was also supported in part by the Intramural Research Program of the National Institutes of Health, National Cancer Institute, Center for Cancer Research.

* Correspondence should be addressed to this author. Phone: (402)-472-4948. Fax: (402)-472-7842 E-mail: vgladyshev1@unl.edu.

[‡] Department of Biochemistry, University of Nebraska.

[§] NTNU.

^{||} National Institutes of Health.

[⊥] Department of Chemistry, University of Nebraska.

[#] University of Texas Southwestern Medical Center.

[▽] Warsaw University.

¹ Abbreviations: SelW, selenoprotein W; SelT, selenoprotein T; SelH, selenoprotein H; Sec, selenocysteine; GPx1, glutathione peroxidase 1; Sep15, 15 kDa selenoprotein; DTT, dithiothreitol; *trsp*, Sec tRNA^{[Ser]Sec} gene; G37*trsp*[†], A37→G37 Sec tRNA^{[Ser]Sec} transgene; *AlbCre*, albumin promoter; CxxC motif, two cysteines separated by two residues; CxxU motif, cysteine and selenocysteine separated by two residues.

SelV is a larger protein than SelW having a short C-terminal SelW homology domain and a longer N-terminal sequence with no close homologues in sequence databases (7). SelH (a homologue of *Drosophila* BthD (13)) was recently found to reside in nucleoli and predicted to possess a thioredoxin-like fold (14). No functional information is available for SelT (15), whereas SelM was found to be distantly related to another mammalian selenoprotein, the 15 kDa selenoprotein (Sep15) (16). The structures of Sep15 and SelM have recently been solved establishing these proteins as endoplasmic reticulum-resident redox proteins (17).

In this work, we used sensitive sequence searches to define a new selenoprotein family, which includes four mammalian selenoproteins: SelT, SelW, SelV, and SelH. Additional members of this family are eukaryotic, bacterial, and archaeal proteins, as well as a protein, designated Rdx12, with Sec in fish and Cys residue in mammalian orthologues. We cloned and characterized three mammalian members of this family.

MATERIALS AND METHODS

Materials. Restriction enzymes were from Fermentas. PCR kits were from Stratagene and Invitrogen. Bacterial cells (NovaBlue, BL21(DE3), Rosetta(DE3), and Rosetta-gami 2(DE3)) were from Novagen. Lipofectamine Plus was from Invitrogen. Other reagents were from Sigma.

Sequence Searches and Multiple Sequence Alignment. Exhaustive, transitive sequence searches were performed with PSI-BLAST (18) run against the NCBI non-redundant protein sequence database with *E*-value threshold of 0.01. Multiple sequence alignment for collected Rdx family proteins was prepared using PCMA program (19) followed by manual adjustments according to the structure of one of the family members (pdb|2fa8).

Cloning and Site-Directed Mutagenesis. Mouse SelW, SelT, and Rdx12 cDNAs were amplified from EST clones (accession numbers gi 22341839, gi 20353091, and gi 18204560, respectively) and cloned into the following vectors: pET21b and pET28a (Novagen) for expression in bacterial cells, and pEGFP-N2, pEGFP-C3 (Clontech), and pCMV-Tag2B (Stratagene) for expression in mammalian cells. The following primers were used for bacterial expression: GGAGCGGGCACATATGAGTGGGGAGC-CAGCGCCGGTGTGTC and ATCATTCTCTCGAGCAG-GATGACACAGGGAGGCCGGCTG for Rdx12 (insertion at *Nde*I and *Xho*I sites); TGCGACGTGCACATATG-GCGCTCGCCGTTTCGAGT and CCTGCCTCTAGCTC-GAGCTGGCACTGAGCCAAGGCAGC for SelW (insertion at *Nde*I and *Xho*I sites); and CAGCAAGAGAGC-TAGCATGCAGTACGCCACCGG and GCTGATAGG-TACTCGAGTGATCGATGATGTGGGATTG for SelT (insertion at *Nhe*I and *Xho*I sites). To prepare SelW fused to a FLAG tag, TAAGAAGGAGATGAATTCATGGCGCT-CGCCGTTTCGAGT and TGGTGGTGCTCGAGTAACTG-GCACTGAGCCAAGGCAGC primers were used for insertion of the resulting PCR product into *Eco*RI and *Xho*I sites. To prepare constructs for Rdx12 localization (a GFP fusion construct), the primers were TGGTGGTGCTCGAGTAAC-TGGCACTGAGCCAAGGCAGC and ATCATTCTCG-GATCCGCAGGATGACACAGGGAGGCCGGCTG (for in-

sertion at *Eco*RI and *Bam*HI sites). To prepare a construct coding for a full-size SelT fused to GFP, the primers were TCTGAAGGCGAATTCAGCGGCTGTCTCAATT-ACGATGAGGCTC and TGATAGGTAGGATCCATGATC-GATGATGTGGGATTGAATCC (*Eco*RI and *Bam*HI sites). The SelT truncated at the N-terminus lacked the following N-terminal sequence: MRLLLLLLVAASAVVRSEASAN-LGGVPSKRLK. To prepare such truncated protein fused to GFP, we used primers GCGTGCCCGAGAATTCGAT-TAAAGATGCAGTACGCCACCGGGC and TGATAGG-TAGGATCCATGATCGATGATGTGGGATTGAATCC (*Eco*RI and *Bam*HI sites). Finally, to fuse the N-terminal SelT sequence to GFP, the primers were TCTGAAGGCGAAT-TCAAGCGGCTGTCTCAATTACGATGAGGCTC and CG-GTGGCGTAGGATCCACTTTAATCTCTTGCTGGG-CACGC (*Eco*RI and *Bam*HI sites). Constructs encoding CxxS and SxxC forms (i.e., Ser replaced Cys or Sec) of the proteins were prepared by site-directed mutagenesis using Quick Change Kit (Stratagene). DNA samples were purified using QIAGEN plasmid purification kits. Nucleotide sequences of all constructs were verified by DNA sequencing at the University of Nebraska genomics core facility.

Protein Expression and Purification. Rdx family proteins were initially expressed in *Escherichia coli* and *Saccharomyces cerevisiae*. Transformed cells, containing corresponding expression constructs, were grown at either 30 °C (yeast) or 37 °C (bacteria). For bacterial expression, protein synthesis was induced by addition of 1 mM IPTG. Cells were grown until the optical density reached 1.0–1.1 at 600 nm, harvested by centrifugation at 6,000 rpm for 10 min and stored at –20 °C. The protein purification procedure followed a protocol provided by BD Biosciences for metal affinity resins. Briefly, cells were thawed in 50 mL of 50 mM sodium phosphate, pH 7.5, containing 300 mM sodium chloride. Protease inhibitor cocktail was added to the solution, and the cells were sonicated using a Misonix XL sonicator. The cell extract was centrifuged at 15,000 rpm for 1 h at 4 °C, and the supernatant loaded on a 3 mL Talon Super Flow column (Clontech). The column was washed with 100 mL of 50 mM sodium phosphate, pH 7.5, 300 mM sodium chloride, and the protein was eluted by a solution of 50 mM sodium phosphate, pH 7.5, 300 mM sodium chloride, and 150 mM imidazole. The purity of recombinant protein was analyzed by SDS PAGE.

Protein Expression and Localization in Mammalian Cells. Mammalian cells (NIH 3T3 or CV-1) were transfected with the constructs coding for Rdx family proteins using Lipofectamine Plus following the protocol described by Invitrogen. Transfected cells were incubated overnight at 37 °C in a CO₂ incubator prior to localization experiments. The markers for protein localization were ER Tracker from Molecular Probes and anti-p230 Golgi mouse monoclonal antibody from BD Transduction Labs and donkey anti-mouse Cy5 conjugated antibodies from Chemicon. A BioRad confocal fluorescent microscope was used to determine cellular location of proteins at the University of Nebraska microscopy core facility.

Identification of Target Proteins. Targets for SelW and Rdx12 were identified by trapping mixed disulfides formed between SelW or Rdx12 and protein targets on affinity resins. SelW and Rdx12 affinity resins were prepared by cross-

linking recombinant Rdx proteins (i.e., CxxS and SxxC forms of these proteins) to activated BrCN-Sepharose (Amersham) according to recommendations of the manufacturer. Cytosolic fractions were prepared by differential centrifugation of homogenates in 50 mM Tris-HCl, pH 8.0, and incubated with SelW- or Rdx12-immobilized BrCN-Sepharose resins for 1 h at 25 °C. The resins were extensively washed with 50 mM Tris-HCl, pH 8.0, 200 mM NaCl, to remove non-specifically bound proteins until absorbance of the eluted fraction at 280 nm reached zero. The resins were then resuspended in 50 mM Tris-HCl, pH 8.0, 200 mM NaCl, 10 mM dithiothreitol (DTT), and incubated for 30 min at 25 °C. The eluted samples were concentrated to a final volume of 50–80 μ L, fractionated by SDS PAGE, and proteins stained with Coomassie Blue.

The stained bands were excised and subjected to LC/MS. Briefly, gel pieces were digested by trypsin (Promega, Madison, WI) and the digested peptides were extracted in 5% formic acid/50% acetonitrile and separated using a C18 reversed phase LC column (75 μ m \times 15 cm, Pepmap 300, 5 μ m particle size) (Dionex, Sunnyvale, CA). A Q-TOF Ultima tandem mass spectrometer (Waters) with electrospray ionization was used to analyze the eluting peptides. The system was user controlled employing MassLynx software (v 4.0, Waters) in data-dependent acquisition mode with the following parameters: 1 s survey scan (380–1900 Da) followed by up to three 2.4 s MS/MS acquisitions (60–1900 Da). The instrument was operated at a mass resolution of 8000. The instrument was calibrated using the fragment ion masses of doubly protonated Glu-fibrinopeptide.

The peak lists of MS/MS data were generated with Distiller (Matrix Science, London, U.K.) using charge state recognition and deisotoping with the other default parameters for Q-TOF data. Data base searches with the acquired MS/MS spectra were performed using Mascot (Matrix Science, v1.9.0, London, U.K.). When using the MSDB database (a comprehensive, nonidentical protein sequence database maintained by the Proteomics Department at the Hammer-smith Campus of Imperial College London which combines entries from TREMPL, SWISSPOT, and GENBANK) (Release 02272005, 1,942,918 sequence entries), no taxonomy was specified. Search parameters used were as follows: no restrictions on protein molecular weight or *pI*, enzymatic specificity was set to trypsin, and methionine oxidation was allowed as a variable peptide modification. Mass accuracy settings were 0.15 Da for peptide mass and 0.12 Da for fragment ion masses.

Labeling of Mouse Tissues with ^{75}Se . Experiments involving metabolic labeling of selenoproteins were carried out by adding ^{75}Se (^{75}Se)selenous acid; specific activity, 1,000 Ci/mmol) to the culture media. The isotope was obtained from the Research Reactor Facility, University of Missouri, Columbia, MO, and the experiments were performed as described elsewhere (20).

Immunoblot (Western Blot) Analyses. Immunoblot detection of SelT was performed using previously described anti-SelT antibodies (15). In other assays, primary anti-His-tag (Novagen), anti-14-3-3 (Santa Cruz), and anti-FLAG (Sigma) antibodies, as well as anti-mouse and anti-rabbit secondary antibodies conjugated to horseradish peroxidase (Amersham) were used.

Northern Blot Analyses. Mouse Adult Tissue Blots were purchased from Seegene. Probes were prepared using Rediprime II Random Prime Labeling System (Amersham) according to the manufacturer's protocol. Membranes were hybridized with ^{32}P -labeled (Redivue [^{32}P]dCTP, Amersham) fragments of mouse SelT, Rdx12, and SelW cDNAs corresponding to their coding regions, and autoradiograms generated.

Quantitative PCR. The relative expression of genes was quantified by real-time PCR. The DNA Engine Opticon 2 Real-Time PCR Detection System (MJ-Research/Bio Rad laboratories, Hercules, CA) was used in combination with SelT specific primer sequences (forward, 5'-TGGTCTAAGCTGGAATCTGG-3'; reverse, 5'-TTTCGGTGCTGATAGGTAGG-3'). Two micrograms of total RNA from each tissue was used to synthesize the first strand cDNA in a 20 μ L reaction mixture by using SuperScript II reverse transcriptase enzyme (Invitrogen) and random primers. Twenty nanograms of cDNA was utilized for the PCR reaction, using iQTM SYBR green supermix (Bio Rad laboratories, Hercules, CA) and 500 nM of each primer, under the following conditions: initial denaturation for 5 min at 95 °C, followed by 40 cycles consisting of 20 s at 94 °C, 20 s at 55 °C, and 30 s at 72 °C. Amplifying known amounts of a PCR-product generated a standard curve at the same time as the samples. The expression of mRNA in each sample was normalized to the expression of 18S rRNA.

Immunoprecipitation Experiments. NIH 3T3 cells were washed twice with PBS, 700 μ L of a lysis buffer containing protease inhibitors added, and the sample kept at 4 °C with continuous shaking for 30–45 min. The soluble fraction was collected by centrifugation at 12,000 rpm for 15 min at 4 °C, and the supernatant stored at –80 °C. Immunoprecipitation experiments were performed using a Protein G immunoprecipitation kit (Sigma) following the protocol provided by the manufacturer. The presence of 14-3-3 protein among SelW protein targets was verified by Western blot analysis using antibodies specific for 14-3-3.

Mouse Models. The mouse lines used in this study have been described elsewhere and are transgenic mice carrying 10 copies of the wild type Sec tRNA^{[Ser]Sec} transgene (*trsp*⁺) or eight copies of the mutant, A37→G37 Sec tRNA^{[Ser]Sec} transgene (G37*trsp*⁺) (20), or are a conditional knockout of the Sec tRNA^{[Ser]Sec} gene (*trsp*^{fl})/transgenic mice carrying the *Cre* recombinase transgene under the control of the albumin promoter (*AlbCre*) (21). The latter mouse is designated Δ *trsp-AlbCre* as it lacks *trsp* (the Sec tRNA^{[Ser]Sec} wild type gene) in liver (22) and retains the *AlbCre* transgene. Matings between Δ *trsp-AlbCre* and either *trsp*⁺ or G37*trsp*⁺ to obtain a mouse line in which selenoproteins have been rescued in liver are similar to those employed previously in generating a mouse line wherein a standard knockout of *trsp* was complemented by either *trsp*⁺ or G37*trsp*⁺ (22, 23). The only difference in obtaining the mouse line used in the present study in which selenoproteins were rescued in liver is that another transgene (*AlbCre*) must be included in the genotype along with Δ *trsp* and either *trsp*⁺ or G37*trsp*⁺. Genotyping of mouse lines to identify each gene, *trsp* (21, 22), *trsp*⁺ (20, 22), G37*trsp*⁺ (20, 22), Δ *trsp* (21), and *AlbCre* (21), have been detailed in the references as indicated.

[illegible]

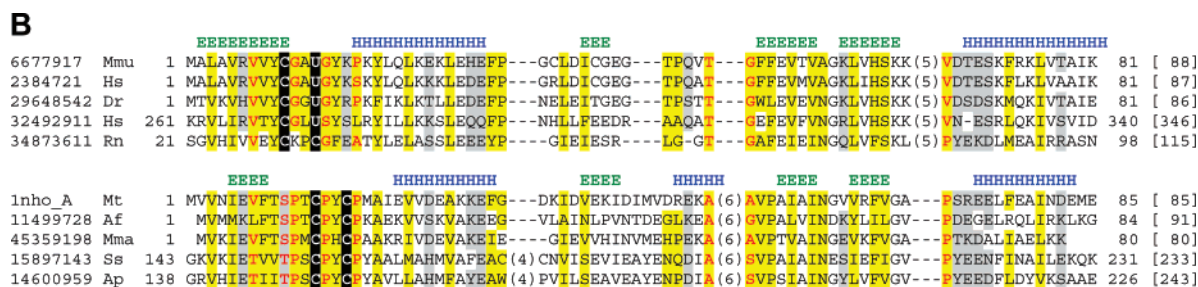


FIGURE 1: Rdx proteins are a family of thioredoxin fold-like proteins. (A) Alignment of SelW, SelV, Rdx12, SelH, and SelT proteins. Representative sequences were aligned with a T-coffee program, following removal of the SelT sequences containing helical insertion (this region is shown in the inset in the figure). Protein designation and sources of sequences are shown on the left side of the figure. Sec (U) is shown in red and Cys in blue in the predicted active site. Conserved residues are highlighted using BoxShade program v3.21. Locations of the predicted secondary structure elements (E, β -strand; H, α -helix) are shown above the sequences. (B) Alignment of Rdx proteins and other thioredoxin fold-like proteins. Sequences are labeled according to the NCBI gene identification (gi) number or PDB code and an abbreviation of the species name: Af, *Archaeoglobus fulgidus*; A, *Aeropyrum pernix*; Dr, *Danio rerio*; Hs, *Homo sapiens*; Mma, *Methanococcus maripaludis*; Mmu, *Mus musculus*; Mt, *Methanobacterium thermoautotrophicum*; Rn, *Rattus norvegicus*; and Ss, *Sulfolobus solfataricus*. The first and last residue numbers are indicated before and after each sequence with the lengths of insertions specified in parentheses. The total length of each sequence is shown in square brackets at the end of the alignment. Residue conservation is denoted with the following scheme: uncharged residues in mostly hydrophobic positions are highlighted in yellow; charged and polar residues in mostly hydrophilic positions are highlighted in gray; small residues at positions occupied mostly by small residues are shown in red. Invariant Cys (C)/Sec (U) residues are highlighted in black. Locations of the predicted (gi 6677917) and observed (1nho_A) secondary structure elements (E, β -strand; H, α -helix) are marked above the sequences.

RESULTS AND DISCUSSION

Mammalian SelT, SelW, SelH, and SelV Selenoproteins Are Distant Homologues. Several mammalian selenoprotein families have Sec separated by 0–2 residues from a conserved Cys. Among these, SelT, SelW, SelH, and SelV contain a CxxU motif. The presence and location of the CxxU motif between a predicted β -strand and an α -helix suggested analogies to redox proteins of the thioredoxin fold. Many thioredoxin fold proteins, such as thioredoxins, glutaredoxins, and protein disulfide isomerases, use CxxC motifs for various redox functions (24).

Pairwise sequence alignments involving mammalian SelW, SelT, SelH, and SelV selenoproteins revealed no significant similarity among these proteins, except for SelV and SelW proteins which have a common SelW homology domain. However, PSI-BLAST search using SelT sequence as a query identified an additional 12 kDa mammalian protein of unknown function, which has a CxxC motif present in place of the CxxU motif in SelT. Here, we designate this protein as Rdx12. Using Rdx12 sequence as a query in further PSI-BLAST searches, several SelW, SelH, and SelV sequences were then detected with an *E*-value below 0.1. Importantly, multiple sequence alignments involving SelT, Rdx12, SelV, SelH, and SelW (Figure 1A) placed CxxU (or CxxC) in the same position in the alignment. Thus, the four selenoprotein families and Rdx12 proteins are members of one larger family. All the proteins have similar patterns of predicted secondary structure with an additional alpha helical insertion unique to SelT (Figure 1A).

Further sequence searches involving Rdx12 proteins identified Sec-containing homologues in fish, including *Tetraodon*, fugu, and zebrafish, as well as predicted selenoprotein homologues represented by ESTs in several other species of fish. Zebrafish Rdx12 sequences were previously designated as SelW2a and SelW2b, but sequence alignments cluster them with mammalian Rdx12 rather than SelW.

The Rdx Family Is a Family of Thioredoxin-like Proteins. Subsequent in-depth, transitive PSI-BLAST searches initiated with *Homo sapiens* SelW (gi 2384721) against the NCBI

non-redundant protein sequence database revealed more than 200 homologous sequences, including Rdx12, SelW, SelV, SelH, and SelT, from various organisms, many hypothetical proteins and a number of prokaryotic proteins belonging to an uncharacterized cluster of orthologues, COG3526 (Figure 1B). We further designate the protein family containing all detected homologues as the Rdx (for redox) family of proteins.

Several fold recognition methods available *via* the protein structure prediction Meta Server consistently assigned thioredoxin fold for both *H. sapiens* (gi 2384721) and *Mus musculus* (gi 6677917) SelW. The highest scoring 3D-Jury hits encompassed matches to a thioredoxin-like protein Mt0807 (25) (PDB accession number 1NHO), including a fair mapping of predicted and observed secondary structure elements. Although some fold recognition servers misaligned (by three residues) two invariant Cys/Sec residues of the proteins of the SelW family with active site cysteines of Mt0807 protein, these residues probably occupy similar positions in protein structure and play similar functional roles.

Furthermore, while our work was in progress, coordinates of a distant SelW homologue from *Agrobacterium tumefaciens* (PDB accession number 2FA8) appeared in the PDB. This structure has a thioredoxin-like fold with an invariant CxxC motif located between first β -strand and α -helix. Transitive PSI-BLAST searches initiated with this sequence against the NCBI non-redundant protein sequence database further confirmed the finding that this protein, four mammalian selenoproteins (SelW, SelT, SelV, and SelH), and Rdx12 were evolutionarily related, although their sequences display limited sequence similarity.

The thioredoxin fold has an α/β structure with the following order of secondary structure elements: β 1- α 1- β 2- α 2- β 3- β 4- α 3 (26). The fold allows insertions of additional segments upstream and downstream of the minimal thioredoxin fold, as well as before and after helix 2. An important difference between the classical thioredoxin fold and the fold predicted for Rdx proteins is the absence of helix 2 in at least some of the latter proteins. This helix is also missing

in several other unrelated thioredoxin fold-like proteins, as well as in selenoproteins Sep15 and SelM (17). The α -helical insertion in SelT (according to secondary structure predictions) corresponds to the location of the disposable thioredoxin fold helix (Figure 1).

Based on the sequence and structure data, Rdx is a family of thioredoxin-like proteins that contain CxxU or CxxC motifs. An additional feature of these proteins is a conserved stretch of amino acids in the middle or C-terminal regions (depending on protein) with the following consensus sequence: tGxFEI(V), where capital letters correspond to highly conserved residues, small letters to the residues most often observed in the indicated position, and x to any residue. Thioredoxins, glutaredoxins, GSTs, GPxs, and many other thioredoxin fold proteins, while with all likelihood being homologous to Rdx proteins, are excluded from this family due to much lower sequence similarity and the lack of the tGxFEI(V) motif. All members of the Rdx family, including a more distantly related SelH, show sequence similarity and have the same conserved region in the C-terminal portion of the protein.

Preparation of Recombinant Proteins of the Rdx Family. The evidence of the thioredoxin-like fold in Rdx selenoproteins and their Cys orthologues and homologues suggested a redox function for this protein family. The majority of thioredoxin fold proteins are thiol-based oxidoreductases, such as thioredoxins, glutaredoxins, peroxiredoxins, glutathione peroxidases, and various Dsb proteins (27, 28). To further characterize mammalian members of this family, we cloned mouse SelT, Rdx12, and SelW and generated various expression constructs for these proteins. To prepare recombinant versions of these proteins, we mutated the Sec codons coding in SelW and SelT to Cys codons, whereas the natural (CxxC) form of Rdx12 was used. In addition, we prepared mutant constructs coding for protein forms, which replaced one of the candidate redox residues in the CxxC (or CxxU) motif with Ser (e.g., CxxS and SxxC forms of each protein).

Mouse SelW with a His-tag at the C-terminus was abundantly expressed in *E. coli* BL21 cells, and a pure protein was obtained by a one-step affinity purification procedure. About 50 mg of protein per liter of culture medium could be obtained for both SxxC and CxxS forms of the protein. In contrast, both CxxS and SxxC forms of SelT were expressed at a very low level in BL21(DE3) cells. These proteins could only be detected with antibodies specific for the C-terminal peptide of SelT (data not shown). The use of other bacterial cells (i.e., Rosetta and Rosetta-gami 2) did not result in any significant increase in protein yield. We also attempted to express SelT in yeast cells, but again the protein could be expressed only at a very low level (data not shown). Thus, SelT either manifested an apparent toxicity or was highly unstable in both bacterial and yeast cells.

Like SelT, Rdx12 could not be overexpressed in BL21 cells, but Rosetta-gami 2 (DE3) cells efficiently synthesized the recombinant protein. We prepared both CxxS and SxxC forms of His-tagged Rdx12 by affinity chromatography with a yield of 1.5–2.0 mg of protein per liter of culture medium. All forms of recombinant Rdx12 and SelW were soluble proteins and had no visible absorbance corresponding to bound cofactors.

Tissue Distribution of SelT, SelW, and Rdx12. To characterize expression of the Rdx mRNAs in mouse tissues,

we carried out Northern blot assays. Signals were detected in all tissues examined (Figure 2). SelT mRNA was expressed at the highest level in kidney, followed by brain, heart, and thymus, whereas Rdx12 mRNA was most abundant in kidney, followed by brain and testis tissues. SelW mRNA was predominantly expressed in brain, skeletal muscle, and testis (Figure 2A). The latter data are in agreement with previous analyses of SelW mRNA expression (5, 9–11). In addition to Northern blot assays, we examined SelT expression by quantitative PCR (Figure 2B). The highest expression level was observed in kidney, followed by brain, heart, and testes. Finally, we analyzed the same organs with regard to SelT expression by Western blot analyses. Again, SelT was detected at the highest levels in testes and kidney (Figure 2C).

Intracellular Localization of Rdx Proteins. It was previously established that SelW is a cytosolic protein (3, 4, 9–11). Therefore, in the present study we focused on the intracellular location of SelT and Rdx12. Rdx12 sequences did not have predicted N-terminal signal sequences. The Rdx12-GFP fusion protein showed the same distribution in transfected NIH 3T3 cells as GFP alone (Figure 3). Therefore, similar to SelW, Rdx12 appears to localize to the cytosol and possibly in the nucleus.

Multiple sequence alignments of Rdx proteins suggested that SelT may have an N-terminal extension, which had characteristics of a signal peptide. To test if the N-terminal sequences of SelT are involved in its subcellular distribution, we prepared various constructs containing SelT-GFP fusion protein, which either had or lacked the N-terminal residues of SelT.

As shown in Figure 4, full-length SelT fused to GFP had an unusual distribution pattern in transfected cells. This distribution was independent of the presence of the N-terminal sequences. In contrast, a protein containing the N-terminal sequence of SelT fused to GFP was distributed throughout the cells, similar to GFP alone. These observations argue against the role of N-terminal sequences in localization of SelT-GFP.

To further localize SelT, double staining of SelT and lysosomes was performed using a marker specific for this compartment, which excluded the presence of SelT in lysosomes (Figure 4). Similarly, we excluded nuclei, peroxisomes, and mitochondria. However, a partial overlap was observed with the Golgi marker. Overall, the data were consistent with localization of SelT in the Golgi with possible occurrence in the ER and cytosol.

Identification of Targets of Rdx12 in Mammalian Cells. The thioredoxin fold and the presence of the CxxC and CxxU motifs in Rdx proteins suggested further analogy to thioredoxins in regard to their thioredoxin reaction cycle mechanisms. During the reaction, thioredoxins first form a transient disulfide with the target protein, followed by attack involving a second Cys of the CxxC motif to form a reduced target and oxidized thioredoxin (24, 27, 28). Mutation of the resolving Cys can stabilize the transient intermolecular disulfide bond and allow selective binding of targets to thioredoxins (29). Similarly, to stabilize transient intermolecular disulfides and utilize this property to trap target proteins, we mutated the redox motifs in Rdx family members to replace one of the Cys (or Sec) with Ser. We also separately mutated another Cys in the motif because it

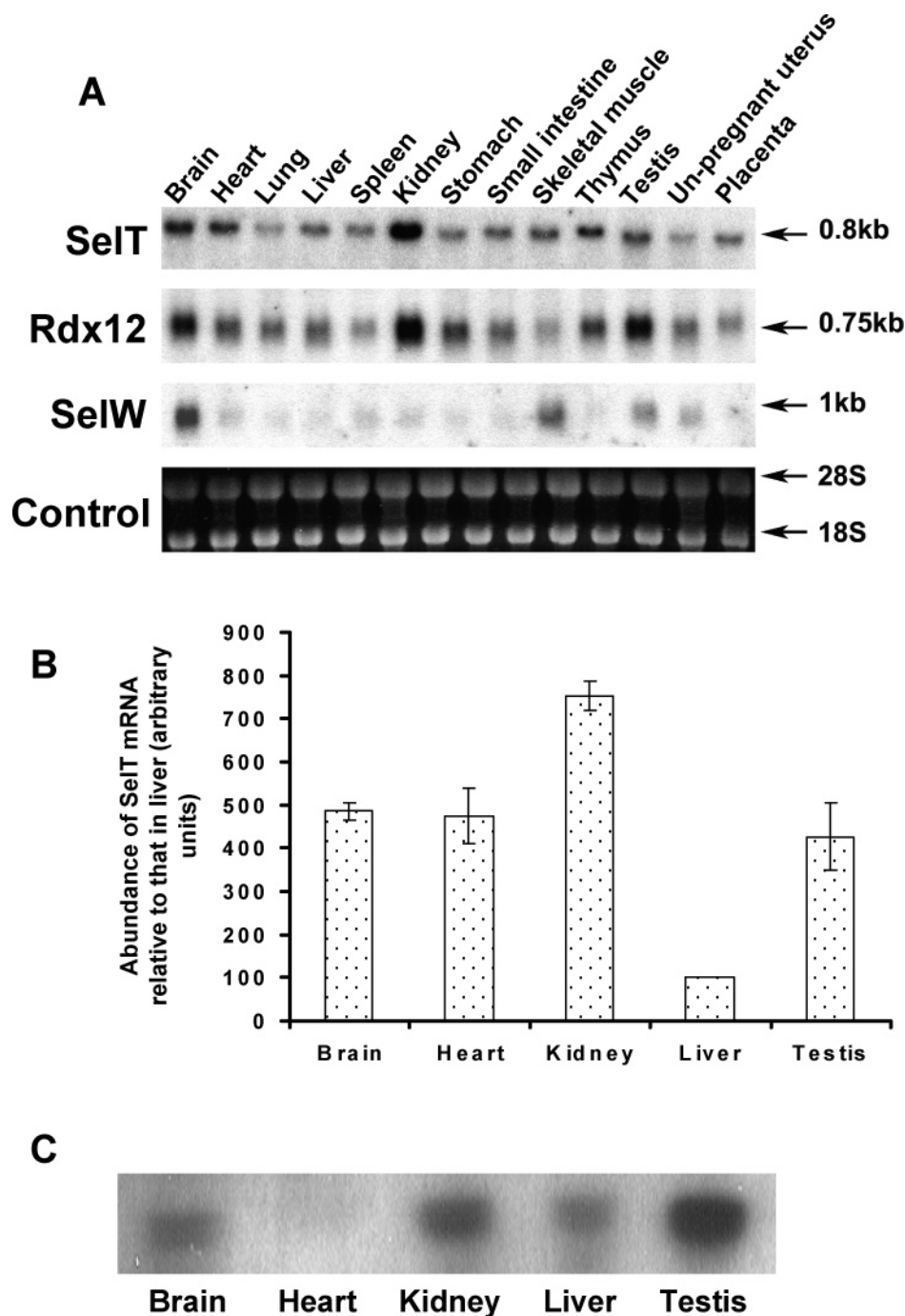


FIGURE 2: Expression of Rdx proteins in mouse tissues. (A) Northern blot analysis of premade membranes containing mRNA (20 μ g per lane) from indicated adult mouse tissues for SelT (first panel), Rdx12 (second panel), and SelW (third panel). The fourth panel shows 18S and 28S ribosomal RNA as loading controls. (B) Determination of SelT mRNA expression levels in indicated mouse tissues by quantitative PCR. Each sample was done in triplicate, and error bars represent the standard deviation. (C) Western blot analysis of SelT expression in indicated mouse tissues. Ten micrograms of proteins was loaded in each lane.

was not known *a priori* which Cys (or Sec) is the attacking or resolving residue. The use of the two mutant variants provided important controls.

The CxxS and SxxC forms of Rdx12 were purified to homogeneity and immobilized on cyanogen bromide-activated Sepharose resins. Cytosolic liver tissue extracts were chosen for target search experiments. A silver stained SDS PAGE gel showing proteins eluted from CxxS-Rdx12 and SxxC-Rdx12 resins is presented in Figure 5A. The stained protein bands, which were enriched with respect to the initial crude extract sample, were excised from the gel

and analyzed by mass spectrometry sequencing, and the sequences detected were analyzed by TBLASTN against NCBI mouse genome and proteome databases. The same set of target proteins was identified for each (i.e., CxxS and SxxC) Rdx12 form.

The most abundant band in Figure 5A corresponded to Rdx12 itself, which was eluted in small amounts from the affinity matrix. The band A1 consisted of three protein targets: glutathione peroxidase 1 (GPx1), peroxiredoxin 1, and glutathione-S-transferase. To elucidate the specificity of these interactions, we directly examined the

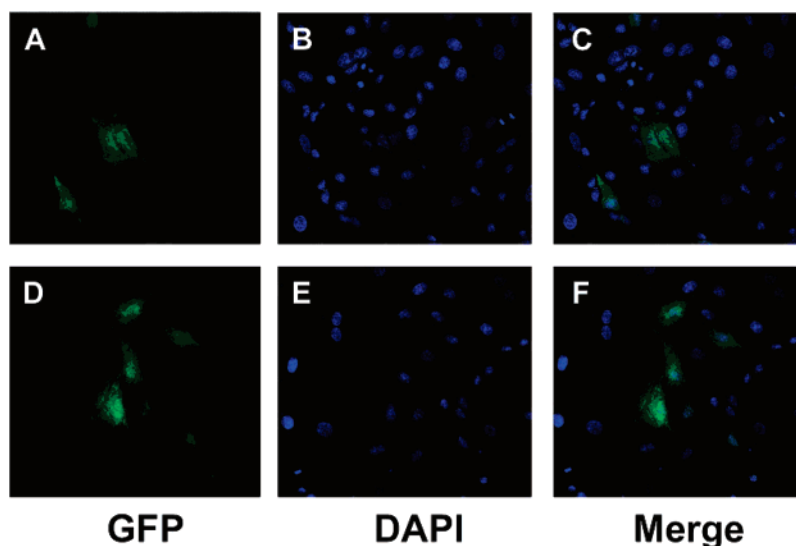


FIGURE 3: Localization of Rdx12-GFP fusion protein in NIH 3T3 cells. Upper panels (A–C) represent confocal images of Rdx12-GFP fusion protein transiently expressed in NIH 3T3 cells. Bottom panels correspond to cells transfected with a GFP vector (control). A and D show GFP fluorescence, B and E show the same cells treated with DAPI (nuclear marker), and images C and F were obtained by merging the left and middle panels as shown in the figure.

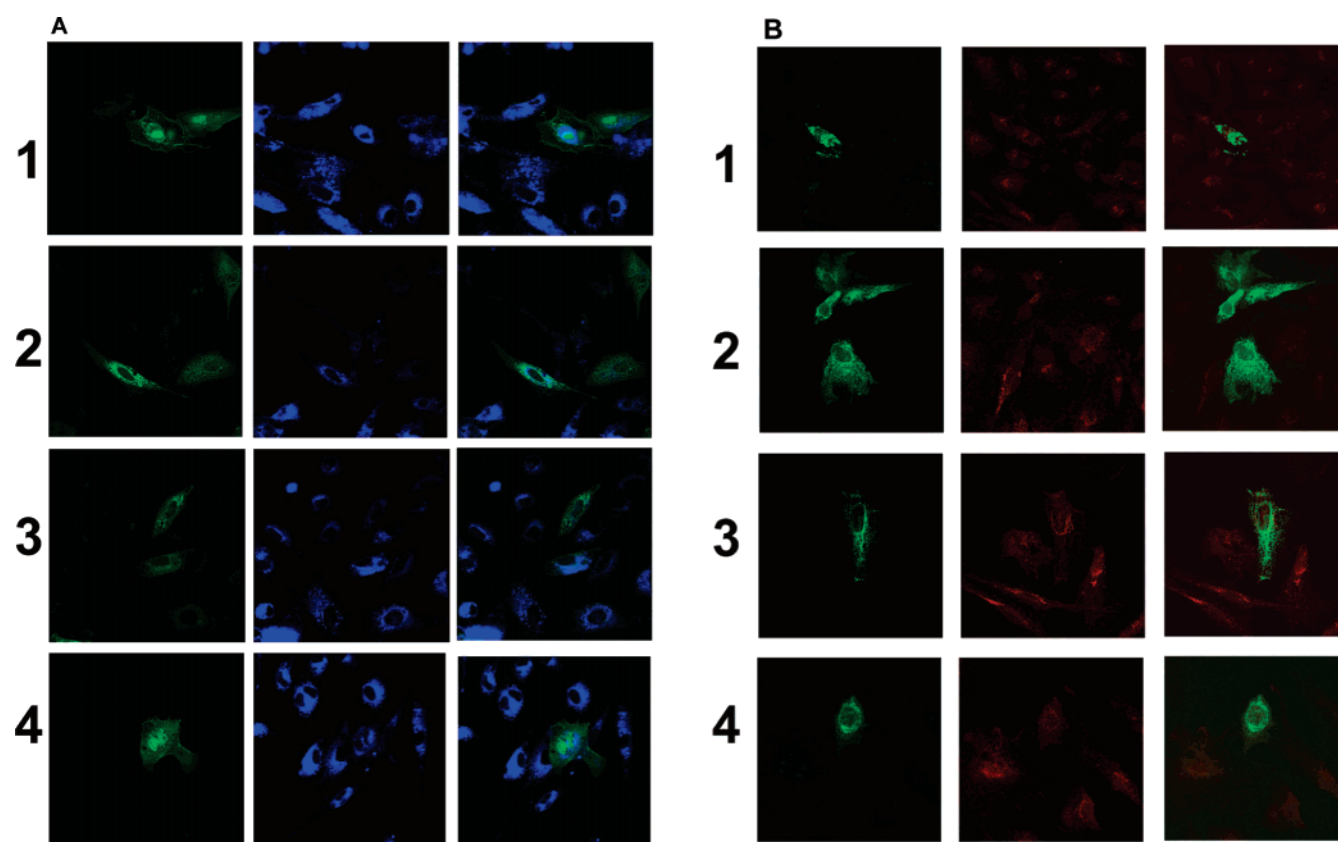


FIGURE 4: Localization of mammalian SelT. (A) SelT localization in NIH 3T3 cells. Confocal images of NIH 3T3 cells expressing various GFP-tagged SelT and control proteins are shown. Each left panel shows green fluorescence corresponding to transiently expressed fusion proteins, each center panel shows fluorescence of the ER Tracker (endoplasmic reticulum marker), and each right panel is an image obtained by merging the left and center panels. 1, N-terminal sequence of SelT fused to GFP; 2, full-length SelT fused to GFP; 3, truncated, N-terminal-less sequence of SelT fused to GFP; and 4, GFP (control). (B) SelT localization in Golgi. Confocal images of NIH 3T3 cells expressing various GFP-tagged SelT and control proteins are shown. Each left panel shows green fluorescence corresponding to transiently expressed fusion proteins, each center panel shows fluorescence of Golgi marker, and each right panel shows an image obtained by merging the left and center panels. Images are organized in the same order as in A.

ability of Rdx12 to bind GPx1 by taking advantage of the fact that GPx1 is a selenoprotein. We carried out the target search using extracts from ^{75}Se -labeled mouse liver and the SxxC form of Rdx12 (Figure 5B). GPx1, the major selenoprotein in mouse liver, migrates as a 25 kDa band.

Comparison of the lanes corresponding to the initial liver extract (lane 1), the flow-through fraction containing proteins that did not bind to the Rdx12 resin (lane 2), and the Rdx12-bound proteins which were eluted from the resin with a reducing agent DTT (lane 3) revealed that GPx1 was

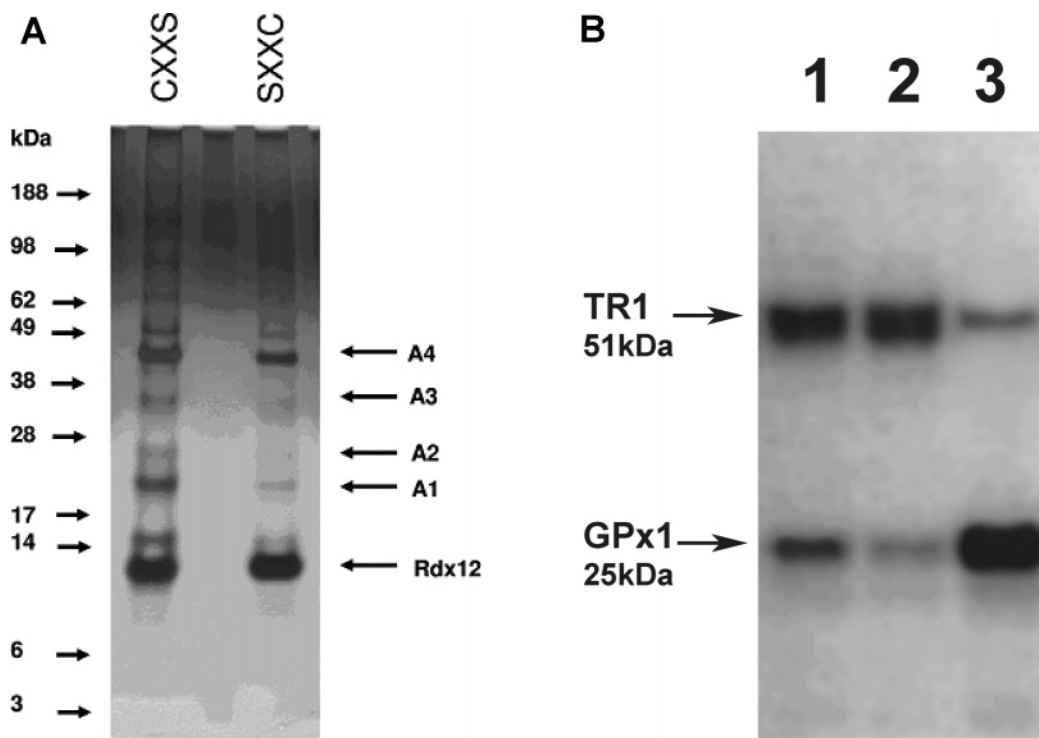


FIGURE 5: Identification of Rdx12 target proteins in mouse liver. (A) A silver stained SDS PAGE gel shows “pull down” experiments involving CxxS and SxxC forms of Rdx12. Due to close similarity of targets identified for each of the variants, the targets are labeled only for the CxxS mutant. Location of molecular weight standards (in kDa) are also shown. (B) Enrichment experiment involving ^{75}Se -labeled mouse liver. Lane assignments are as follows: 1, initial liver extract; 2, flow-through fraction containing proteins that did not bind to the Rdx12 resin; and 3, Rdx12-bound proteins which were eluted from the resin with DTT. Location of GPx1, which is the major ^{75}Se -labeled protein in liver, is indicated.

significantly enriched on the Rdx12 resin, indicating that GPx1 is an Rdx12 binding partner. Other identified protein targets were carbonic anhydrase (band A2), betaine S-methyltransferase (band A3), and selenium binding protein 2 (band A4).

Identification of Targets of SelW. A similar procedure was used to identify targets of SelW. However, in this case, mouse brain was used as a source of targets because SelW mRNA was found to be abundant in this organ (Figure 2C). A silver stained SDS PAGE gel containing target proteins enriched on the SelW affinity resins from the brain homogenate is shown in Figure 6. The target proteins were identified as peroxiredoxin 1 (band B1), 14-3-3 (band B2), tubulin (band B3), dihydropyrimidinase-related protein-2 (band B4), and heat shock proteins 70 (band B5) and 90 (band B6).

Similar results were obtained when mouse heart was used as the source of SelW targets. In this case, peroxiredoxin 1 and 14-3-3 were identified as the major targets, and heat shock proteins 70 and 90 were also detected by mass spectrometry sequencing (data not shown). Almost complete correspondence between the targets found in mouse brain and heart suggests that SelW may have the same protein partners in both tissues. It should be noted that many SelW and Rdx12 targets enriched on the affinity columns were different, yet both sets included proteins known to serve as oxidoreductases and be redox regulated.

As shown above, one of the SelW target proteins was 14-3-3 protein. Although specific functions of 14-3-3 proteins are not fully understood (30), this family of proteins that includes a number of isoforms and isoproteins are known to

be involved in important cellular processes. 14-3-3 was previously reported to be a target of thioredoxin and peroxiredoxin (31,32), which is consistent with the redox nature of SelW/14-3-3 interactions that we observed. Furthermore, peroxiredoxin itself was found as a SelW target. Therefore, our study complements the list of known 14-3-3 targets, including proteins involved in stress and checkpoint responses (31) and metabolic proteins (32). Our affinity “pull down” data were further examined by analyzing 14-3-3 structures, which revealed that 14-3-3 (e.g., PDB accession number 1A40) has an exposed Cys residue on its surface, which could potentially be involved in redox interaction with SelW.

We further examined whether SelW affinity resins could deplete 14-3-3 from protein homogenates. Brain lysate was incubated with the SelW resins, and the enrichment of 14-3-3 on the SelW affinity resins was verified by Western blot assays (Figure 7A). Comparison of lanes 2 and 3 in Figure 7A shows that 14-3-3 was enriched on the SxxC resin.

Since the 14-3-3 antibodies utilized in this study recognize all 14-3-3 isoforms, further studies will be needed to determine the specificity of SelW interactions with different 14-3-3 proteins. Analysis of primary sequences of 14-3-3 isoforms and peptide sequences detected by mass spectrometry suggests that the 14-3-3 proteins bound to the SelW resin were most likely the eta, beta, zeta, gamma, or tau forms.

To further examine whether SelW and 14-3-3 proteins interact at physiological concentrations, we carried out immunoprecipitation experiments. The constructs coding for CxxS and SxxC forms of SelW were prepared with a

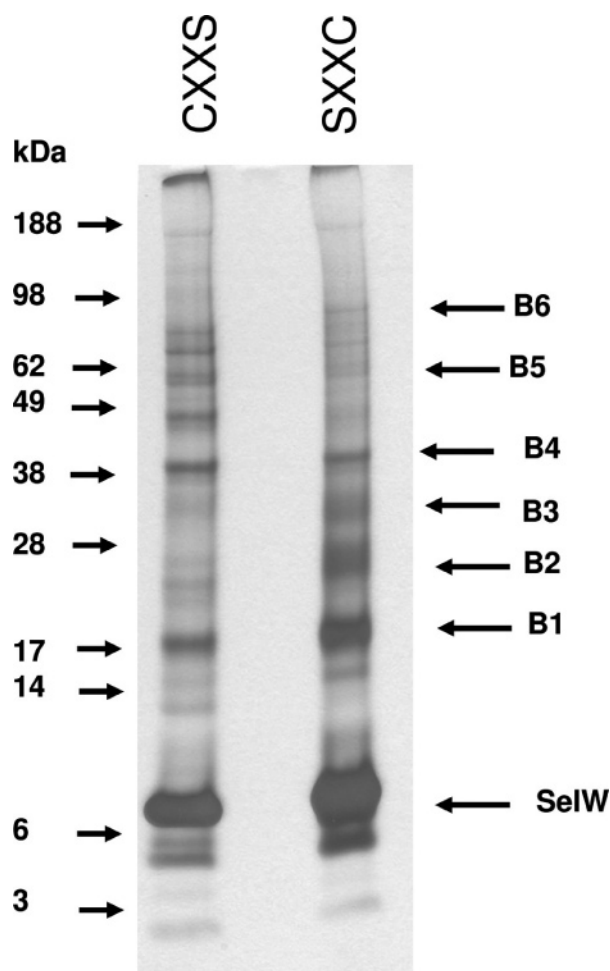


FIGURE 6: Identification of SelW target proteins in mouse brain. Silver stained SDS PAGE gel shows “pull down” experiments using CxxS and SxxC forms of SelW. The target proteins found for the SxxC form are labeled. For comparison, SDS PAGE gel of the mouse brain cytosol is shown. Migration of molecular weight standards is indicated. Lane assignments are as follows: 1, CxxS mutant; and 2, SxxC mutant.

C-terminal FLAG-tag and transfected into NIH 3T3 cells. The cells were lysed in the presence of protease inhibitors and initially examined for expression of SelW and 14-3-3 proteins using anti-FLAG and anti-14-3-3 antibodies, respectively. While both SelW mutant forms could be detected, the endogenous 14-3-3 was not. To overcome this problem, the immunoprecipitation assay was performed using SelW-containing cell lysates and 14-3-3-containing mouse brain cytosol.

SelW was immunoprecipitated from the samples with anti-FLAG antibodies, and the bound proteins were examined for the presence of 14-3-3 (Figure 7B). Both forms of SelW were found to bring down 14-3-3. Comparing the amount of 14-3-3 observed on Western blots for each of the SelW forms with that observed in the initial sample, we estimate that ~4–6% of 14-3-3 could be immunoprecipitated by SelW. As control, the samples were tested for the presence of actin. Figure 7B (lower panel) shows that the immunoprecipitated samples did not contain actin, while this protein was abundant in the initial sample. Thus, it appears that 14-3-3 specifically interacts with both forms of SelW at close to physiological concentrations of both proteins. The patterns of interaction of CxxS and SxxC forms of SelW observed

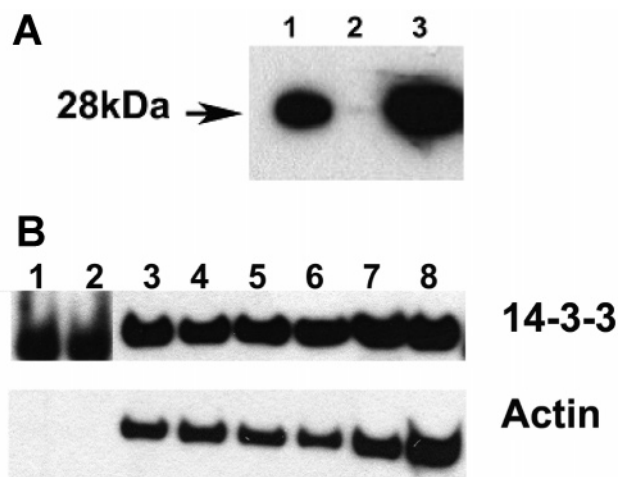


FIGURE 7: Analysis of SelW/14-3-3 interactions. (A) Affinity depletion of 14-3-3 using a SelW resin. Cytosolic extract from mouse brain was incubated with the affinity resin containing the SxxC form of SelW, and bound and unbound fractions were probed in Western blot assays with anti-14-3-3 antibodies. Lane assignments are as follows: 1, mouse brain cytosol; 2, the sample following the pass through the resin; and 3, proteins eluted from the resin following incubation. (B) Western blot analysis of 14-3-3 protein. SxxC and CxxS forms of SelW-FLAG that were immunoprecipitated with anti-FLAG antibodies from transfected NIH 3T3 cells, and the samples were probed with anti-14-3-3 monoclonal antibodies (upper panel) and anti-actin polyclonal antibodies (second panel). Lane assignments are as follows: 1, proteins immunoprecipitated from cells transfected with the CxxS form of SelW; 2, proteins immunoprecipitated from cells transfected with the SxxC form of SelW; 3, sample prior to immunoprecipitation (an initial sample containing the cell lysate and the CxxS form of SelW); 4, an initial sample containing the cell lysate and the SxxC form of SelW; 5, proteins unbound to the CxxS variant; 6, proteins unbound to the SxxC variant; 7, mouse brain cytosol; and 8, NIH 3T3 cell lysate alone.

in “pull down” and immunoprecipitation experiments suggest that, besides the interaction involving intermolecular disulfide bonds, SelW and 14-3-3 could interact in a nonredox manner. The difference between the fraction of 14-3-3 bound to the SelW affinity resin (almost complete depletion) and that immunoprecipitated with SelW-FLAG (4–6% depletion) could be explained by an excess of the affinity resin in the experiment shown in Figure 7A compared to the more physiological situation shown in Figure 7B. Taken together, our data suggest that 14-3-3 is a functional partner of SelW.

The observed SelW/14-3-3 binding is likely noncanonical. Previous studies on interactions of 14-3-3 protein isoforms with their targets provided evidence that 14-3-3 target proteins have to be in the phosphorylated forms (33, 34). Moreover, the 14-3-3 target proteins must contain two canonical binding motifs required for such protein interaction. These motifs are defined as R(S/X)XpSXP and RXXXpSXP, where X denotes any amino acid residue and pS a phosphorylated serine (35). These two features were almost invariably observed for all 14-3-3 protein targets. However, SelW does not contain candidate 14-3-3 interaction motifs. Instead, we hypothesize that SelW regulates 14-3-3 in a redox manner: in the oxidized form (e.g., with a disulfide or a glutathionylated cysteine), 14-3-3 may be inactive and require the reduced form of SelW for activation. Determination of the three-dimensional structure of the SelW/14-3-3 complex would be a key step in

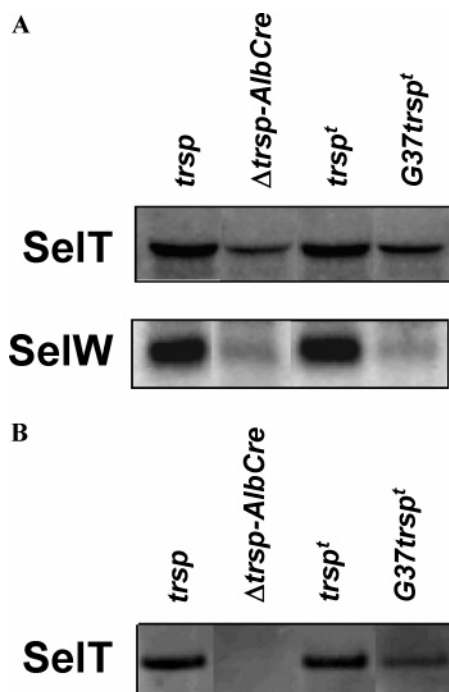


FIGURE 8: Regulation of expression of SelT and SelW in mouse models of disrupted hepatic selenoprotein expression. The mouse models include *trsp*, wild type; $\Delta trsp-AlbCre$, liver selenoprotein knockout; *trsp^f*, liver selenoprotein knockout rescued with wild type transgenes; and *G37trsp^f*, liver selenoprotein knockout rescued with G37 mutant *trsp* transgenes (see text and Materials and Methods for details). (A) Northern blot analyses of SelT and SelW expression in livers of different mouse models of disrupted hepatic selenoprotein expression. (B) Western blot analysis of SelT expression in livers of different mouse models of disrupted hepatic selenoprotein expression.

understanding the physiological function and structural basis of this interaction.

Regulation of SelT and SelW Expression in the Mouse Models of Disrupted Hepatic Selenoprotein Expression. To elucidate the regulation of expression of selenoproteins within the Rdx12 family, we employed mouse models that targeted the removal of selenoprotein expression in liver (21) and carried a mutant tRNA^{[Ser]Sec} (*G37trsp^f*) or wild type (*trsp^f*) transgenes (20) (Figure 8), where *G37trsp^f* designates a A37→G37 mutant Sec tRNA^{[Ser]Sec} transgene. The initial mouse line utilized *loxP-Cre* technology wherein mice carried a floxed conditional knockout of the tRNA^{[Ser]Sec} gene (*trsp^f*) and the *Cre* recombinase gene under the control of the albumin promoter (*AlbCre*) (21). We crossed mice lacking selenoprotein expression in their livers, ($\Delta trsp-AlbCre$) (23), with transgenic mice carrying either *trsp^f* or *G37trsp^f* and subsequently generated mouse lines dependent on *trsp^f* or *G37trsp^f* for selenoprotein expression in their livers (see Materials and Methods). *G37trsp^f* expresses a Sec tRNA^{[Ser]Sec} isoform that supports the synthesis of selenoproteins involved in housekeeping functions (e.g., cytosolic and mitochondrial thioredoxin reductases, and GPx4), whereas the isoform that is involved in the synthesis of stress-related selenoproteins is not expressed (22, 23).

As shown in Figure 8A, SelT and SelW mRNAs were fully recovered in liver of $\Delta trsp-AlbCre$ mice rescued with *trsp^f* (compare lanes 1 and 3). The level of expression of SelT mRNA was reduced in the liver of $\Delta trsp-AlbCre$ mice (compare lanes 1 and 2) and enriched only slightly, if at all,

in the *G37trsp^f* rescued mice (compare lanes 2 and 4). The expression of SelW mRNA, on the other hand, was virtually abolished in $\Delta trsp-AlbCre$ mice and *G37* rescued mice. The tRNA-dependent changes in selenoprotein gene expression were likely due to inability to use mutant tRNA for translation and consequent degradation of untranslated messages.

SelT expression was also examined by Western analysis (Figure 8B). SelT was not expressed in the liver of $\Delta trsp-AlbCre$ mice (lane 2), but was fully expressed in the liver of *trsp^f* mice (lane 3), and only partially expressed in the *G37trsp^f* rescued mice (lane 4). Although the expression of SelW was not examined by Western blotting, it would not be expected to be expressed in the *G37trsp^f* rescued mice since the corresponding mRNA was not synthesized in the $\Delta trsp-AlbCre$ or *G37trsp^f* rescued mice.

The pattern of expression of SelW would suggest that its synthesis is similar to that of GPx1, GPx3, and MsrB1 which were not rescued in a standard knockout mouse that had been rescued with *G37* transgenes (22, 23). SelT was also poorly expressed in the present study as well as in a previous study (22) suggesting that its synthesis is also dependent on the tRNA^{[Ser]Sec} isoform that supports the synthesis of selenoproteins involved in stress-related phenomena.

CONCLUSIONS

In this work, we defined a new family of proteins, designated Rdx, which has high representation of Sec-containing proteins. Four (SelT, SelW, SelH, and SelV) of the 25 human selenoproteins are members of this family, along with an additional fish selenoprotein (Rdx12) and its mammalian Cys homologue. Assignment of thioredoxin fold to the family members together with identified invariant active site CxxU/CxxC motifs suggests a redox function of Rdx proteins. Specific redox targets of Rdx proteins are probably numerous, and in this work, we found that SelW interacts with 14-3-3 and Rdx12 with GPx1. Rdx family members are present in various organs and tissues in mice and localize to different compartments in mammalian cells. Selenoprotein members of this family were found to be regulated by the status of the Sec insertion machinery. Finally, our work provides a basis for further functional analyses of Rdx proteins.

REFERENCES

- Hatfield, D. L., Berry, M. J., and Gladyshev, V. N. (2006) *Selenium: Its molecular biology and role in human health*, Springer Science+Business Media, LLC, New York, NY.
- Stadtman, T. C. (1996) Selenocysteine, *Annu. Rev. Biochem.* 65, 83–100.
- Copeland, P. R., and Driscoll, D. M. (2001) RNA binding proteins and selenocysteine, *Biofactors* 14, 11–16.
- Hoffmann, P. R., and Berry, M. J. (2005) Selenoprotein synthesis: a unique translational mechanism used by a diverse family of proteins, *Thyroid* 15, 769–775.
- Hatfield, D. L., Carlson, B. A., Xu, X. M., Mix, H., and Gladyshev, V. N. (2006) Selenocysteine incorporation machinery and the role of selenoproteins in development and health, *Prog. Nucleic Acid Res. Mol. Biol.* 81, 97–142.
- Castellano, S., Lobanov, A. V., Chapple, C., Novoselov, S. V., Albrecht, M., Hua, D., Lescure, A., Lengauer, T., Krol, A., Gladyshev, V. N., and Guigo, R. (2005) Diversity and functional plasticity of eukaryotic selenoproteins: identification and characterization of the SelJ family, *Proc. Natl. Acad. Sci. U.S.A.* 102, 16188–16193.

7. Kryukov, G. V., Castellano, S., Novoselov, S. V., Lobanov, A. V., Zehab, O., Guigo, R., and Gladyshev, V. N. (2003) Characterization of mammalian selenoproteomes, *Science* 300, 1439–1443.
8. Whanger, P. D. (2000) Selenoprotein W: a review, *Cell. Mol. Life Sci.* 57, 1846–1852.
9. Beilstein, M. A., Vendeland, S. C., Barofsky, E., Jensen, O. N., and Whanger, P. D. (1996) Selenoprotein W of rat muscle binds glutathione and an unknown small molecular weight moiety, *J. Inorg. Biochem.* 61, 117–124.
10. Gu, Q. P., Beilstein, M. A., Barofsky, E., Ream, W., and Whanger, P. D. (1999) Purification, characterization, and glutathione binding to selenoprotein W from monkey muscle, *Arch. Biochem. Biophys.* 361, 25–33.
11. Vendeland, S. C., Beilstein, M. A., Chen, C. L., Jensen, O. N., Barofsky, E., and Whanger, P. D. (1993) Purification and properties of selenoprotein W from rat muscle, *J. Biol. Chem.* 268, 17103–17107.
12. Gu, Q. P., Sun, Y., Ream, L. W., and Whanger, P. D. (2000) Selenoprotein W accumulates primarily in primate skeletal muscle, heart, brain and tongue, *Mol. Cell. Biochem.* 204, 49–56.
13. Castellano, S., Morozova, N., Morey, M., Berry, M. J., Serras, F., Corominas, M., and Guigo, R. (2001) In silico identification of novel selenoproteins in the *Drosophila melanogaster* genome, *EMBO Rep.* 2, 697–702.
14. Novoselov, S. V., Kryukov, G. V., Xu, X. M., Carlson, B. A., Hatfield, D. L., and Gladyshev, V. N. (2007) Selenoprotein H is a nucleolar thioredoxin-like protein with a unique expression pattern, *J. Biol. Chem.* 282, 11960–11968.
15. Kryukov, G. V., Kryukov, V. M., and Gladyshev, V. N. (1999) New mammalian selenocysteine-containing proteins identified with an algorithm that searches for selenocysteine insertion sequence elements, *J. Biol. Chem.* 274, 33888–33897.
16. Korotkov, K. V., Kumaraswamy, E., Zhou, Y., Hatfield, D. L., and Gladyshev, V. N. (2001) Association between the 15-kDa selenoprotein and UDP-glucose:glycoprotein glucosyltransferase in the endoplasmic reticulum of mammalian cells, *J. Biol. Chem.* 276, 15330–15336.
17. Ferguson, A. D., Labunsky, V. M., Fomenko, D. E., Arac, D., Chelliah, Y., Amezcua, C. A., Rizo, J., Gladyshev, V. N., and Deisenhofer, J. (2006) NMR structures of the selenoproteins Sep15 and SelM reveal redox activity of a new thioredoxin-like family, *J. Biol. Chem.* 281, 3536–3543.
18. Altschul, S. F., Madden, T. L., Schaffer, A. A., Zhang, J., Zhang, Z., Miller, W., and Lipman, D. J. (1997) Gapped BLAST and PSI-BLAST: a new generation of protein database search programs, *Nucleic Acids Res.* 25, 3389–3402.
19. Pei, J., Sadreyev, R., and Grishin, N. V. (2003) PCMA: fast and accurate multiple sequence alignment based on profile consistency, *Bioinformatics* 19, 427–428.
20. Moustafa, M. E., Carlson, B. A., El-Saadani, M. A., Kryukov, G. V., Sun, Q. A., Harney, J. W., Hill, K. E., Combs, G. F., Feigenbaum, L., Mansur, D. B., Burk, R. F., Berry, M. J., Diamond, A. M., Lee, B. J., Gladyshev, V. N., and Hatfield, D. L. (2001) Selective inhibition of selenocysteine tRNA maturation and selenoprotein synthesis in transgenic mice expressing isopentenyladenosine-deficient selenocysteine tRNA, *Mol. Cell. Biol.* 21, 3840–3852.
21. Carlson, B. A., Novoselov, S. V., Kumaraswamy, E., Anver, M. R., Gladyshev, V. N., and Hatfield, D. L. (2004) Specific excision of the selenocysteine tRNA^{[Ser]Sec} gene in mouse liver demonstrates an essential role of selenoproteins in liver function, *J. Biol. Chem.* 279, 8011–8017.
22. Carlson, B. A., Xu, X. M., Gladyshev, V. N., and Hatfield, D. L. (2005) Selective rescue of selenoprotein expression in mice lacking a highly specialized methyl group in selenocysteine tRNA, *J. Biol. Chem.* 280, 5542–5548.
23. Carlson, B. A., Xu, X. M., Gladyshev, V. N., and Hatfield, D. L. (2005) in *Topics in Current Genetics* (Grosjean, H., Ed.) Vol. 12, pp 431–438, Springer-Verlag, Berlin-Heidelberg, Germany.
24. Martin, J. L. (1995) Thioredoxin—a fold for all reasons, *Structure* 3, 245–250.
25. Amegbey, G. Y., Monzavi, H., Habibi-Nazhad, B., Bhattacharyya, S., and Wishart, D. S. (2003) Structural and functional characterization of a thioredoxin-like protein (Mt0807) from *Methanobacterium thermoautotrophicum*, *Biochemistry* 42, 8001–8010.
26. Qi, Y., and Grishin, N. V. (2005) Structural classification of thioredoxin-like fold proteins, *Proteins* 58, 376–388.
27. Holmgren, A., Johansson, C., Berndt, C., Lonn, M. E., Hudemann, C., and Lillig, C. H. (2005) Thiol redox control via thioredoxin and glutaredoxin systems, *Biochem. Soc. Trans.* 33, 1375–1377.
28. Fernandes, A. P., and Holmgren, A. (2004) Glutaredoxins: glutathione-dependent redox enzymes with functions far beyond a simple thioredoxin backup system, *Antioxid. Redox Signaling* 6, 63–74.
29. Motohashi, K., Kondoh, A., Stumpp, M. T., and Hisabori, T. (2001) Comprehensive survey of proteins targeted by chloroplast thioredoxin, *Proc. Natl. Acad. Sci. U.S.A.* 98, 11224–11229.
30. Yaffe, M. B. (2002) How do 14-3-3 proteins work?—Gatekeeper phosphorylation and the molecular anvil hypothesis, *FEBS Lett.* 513, 53–57.
31. Meek, S. E., Lane, W. S., and Piwnicka-Worms, H. (2004) Comprehensive proteomic analysis of interphase and mitotic 14-3-3-binding proteins, *J. Biol. Chem.* 279, 32046–32054.
32. Pozuelo Rubio, M., Geraghty, K. M., Wong, B. H., Wood, N. T., Campbell, D. G., Morrice, N., and Mackintosh, C. (2004) 14-3-3-affinity purification of over 200 human phosphoproteins reveals new links to regulation of cellular metabolism, proliferation and trafficking, *Biochem. J.* 15, 379–408.
33. Tzivion, G., and Avruch, J. (2002) 14-3-3 proteins: active cofactors in cellular regulation by serine/threonine phosphorylation, *J. Biol. Chem.* 277, 3061–3064.
34. Rosenquist, M., Alsterfjord, M., Larsson, C., and Sommarin, M. (2001) Data mining the Arabidopsis genome reveals fifteen 14-3-3 genes. Expression is demonstrated for two out of five novel genes, *Plant Physiol.* 127, 142–149.
35. Rittinger, K., Budman, J., Xu, J., Volinia, S., Cantley, L. C., Smerdon, S. J., Gamblin, S. J., and Yaffe, M. B. (1999) Structural analysis of 14-3-3 phosphopeptide complexes identifies a dual role for the nuclear export signal of 14-3-3 in ligand binding, *Mol. Cell.* 4, 153–166.

BI602462Q